Multifaceted mRNA analysis using programmed RNA cleavage by *Mucilaginibacter paludis* Argonaute

Lizhi Liu, Eric A. Hunt, Eric J. Wolf, Ivan R. Corrêa Jr., Erbay Yigit, Sebastian Grünberg

Argonaute (Ago) endonucleases are ubiquitous across all domains of life and, like Cas nucleases, can be programmed by guide oligonucleotides to target and cleave specific nucleic acid sequences. However, unlike Cas enzymes, Agos are not restricted by sequence requirements such as protospacer adjacent motifs (PAMs) enhancing their utility as molecular tools. This study demonstrates diverse applications of the DNA-guided RNA-endonuclease *Mucilaginibacter paludis* Argonaute (Mpa Ago) for *in vitro* mRNA processing, e.g., 3' end polishing, and for mRNA analysis in combination with liquid chromatography tandem mass spectrometry (LC-MS/MS). Applications of the latter include the comprehensive assessment of 5' capping efficiency, 3' poly(A) tail length and composition, one-pot multiplexed cleavage for RNA sequencing, modification detection, and fingerprinting.

Main

Like CRISPR-Cas nucleases, Agos are conserved endonucleases that utilize nucleic acid guides to recognize, bind, and cleave their substrates. However, unlike Cas nucleases, Ago proteins are present across all domains of life[1-3]. In eukaryotes, Agos are loaded with small viral RNAs, endogenous miRNAs, or piRNAs, functioning in RNA interference (RNAi) pathways as components of the RNA-induced silencing complex (RISC)[4-8]. They play crucial roles in antiviral defense, posttranscriptional regulation of gene expression, and suppression of transposon activity[9-11].

Prokaryotic Agos (pAgos) are classified into long and short based on their domain architecture[2, 3]. Long pAgos consist of six domains (N-terminal, L1, PAZ, L2, MID, and PIWI) and share structural similarities with eukaryotic Agos (eAgos). However, some long pAgos are catalytically inactive due to disruptions in their catalytic tetrad,

31 DEDX (X = D/H/N/K), which coordinate divalent metal cations, often Mg^{2+}, that are
32 crucial for activity[1, 2, 12-14]. Short pAgos contain only the MID and PIWI domains and lack
33 the ability to cut nucleic acids due to mutations in the catalytic tetrad[15]. Short pAgos and
34 catalytically inactive long pAgos often associate with other effector proteins which
35 function in bacterial defense systems[16]. In contrast, active long pAgos have been
36 reported to be directly involved in cellular defense against foreign genetic elements as
37 well as in genome replication and recombination[12, 17-21].
38 Active pAgos load short guides to form a nucleoprotein complex that
39 subsequently binds and cleaves complementary target sequences between guide
40 nucleotides 10 and 11, resulting in cleavage products with 3'-OH and 5'-phosphate
41 ends[22]. Unlike eAgos, which exclusively bind RNA guides to cleave RNA targets, most
42 known active long pAgos utilize short DNA guides to target DNA sequences[17, 18, 23-30].
43 Few pAgos have been reported to use RNA guides to cleave DNA[14, 31-34], and still fewer
44 using RNA guides to target RNA[33, 35, 36]. Recently, several pAgos have been reported to
45 use DNA guides to preferentially cleave RNA over DNA[28, 37, 38].
46 The ability to direct endonuclease activity to a specific location with short nucleic
47 acid guides makes pAgos highly versatile and valuable molecular tools with many
48 applications in biotechnology. When compared to Cas nucleases, the lack of sequence
49 restrictions such as PAMs and the predominant use of short DNA guides versus RNA
50 guides make pAgos a versatile and economical alternative, especially for *in vitro*
51 applications. DNA-targeting pAgos are already used in the diagnosis of pathogens and
52 disease related rare mutations, DNA assembly, super-resolution microscopy, and the
53 detection of single and double stranded DNA sequences[39]. However, applications that
54 utilize pAgos to specifically target RNA have not yet been reported.
55 In this work, we describe RNA-specific applications of MpaAgo, a DNA-guided
56 pAgo that preferentially targets RNA substrates[37]. We demonstrate that MpaAgo can be
57 used to efficiently cleave a target RNA at 24 sites simultaneously in a multiplex one-pot
58 reaction, allowing for subsequent RNA sequencing using intact mass spectrometry with
59 up to >90% sequence coverage. Custom guide mixtures generating characteristic RNA
60 fragments enable RNA fingerprinting – a fast and unambiguous way to detect and

identify RNAs by liquid chromatography. We also show that MpaAgo can be used in 5' cap analysis of mRNAs, allowing for the precise determination and relative quantification of the cap incorporation in a workflow that can be adapted to virtually any 5' untranslated region (UTR) sequence and can be performed in under one hour. Lastly, we demonstrate that MpaAgo can be guided to and specifically cleave a sequence embedded in the poly(A) tail of an *in vitro* transcribed mRNA to generate mRNA populations with homogenized 3' ends, removing non-templated additions introduced by RNA polymerases. This also allows for the accurate analysis of the poly(A) tail length and identification of unwanted potential extensions.

Results

MpaAgo efficiently and specifically cleaves mRNA

To assess the potential of pAgos to manipulate therapeutically relevant RNA substrates, we sought to determine the specificity and cleavage efficiency of mRNA substrates by MpaAgo, a DNA-guided endoribonuclease from *Mucilaginibacter paludis*. MpaAgo has previously been described as a programmable endoribonuclease with strong guide-mediated substrate specificity that is capable of cleaving RNA substrates of up to 352 nt in length[37]. We tested site-specific RNA cleavage by MpaAgo on two different *in vitro* transcribed (IVT) mRNAs: pSG90 IVT RNA, which represents a shortened version of the replication-competent Sindbis virus genome[40] (1678 nt), and Fluc (*Firefly luciferase*) IVT RNA (1766 nt). We designed 16 nt long 5'-phosphorylated guides targeting unique sequences in the pSG90 and Fluc IVT RNAs, spaced 100 or 72 nt apart throughout the complete mRNA sequences. When cleaving the pSG90 RNA with MpaAgo using single guides in separate reactions, we observed cleavage efficiencies between 71% and 92% compared to a control reaction containing only MpaAgo without guide (Fig. 1A). Compared to pSG90 RNA, MpaAgo displayed a higher cleavage efficiency of Fluc RNA, resulting in near complete cleavage of the substrate mRNA for most guides (Fig. 1B).

89 To challenge MpaAgo further, we tested cleavage of a uridine-depleted version
90 of the human erythropoietin (Epo) IVT RNA with a GC content (excluding the poly(A)
91 tail) of 59% (pSG95; Fig. S1). The ability to cleave GC-rich substrates is a desirable
92 property, as uridine depletion and/or modification has been shown to reduce
93 immunogenicity and is commonly applied to RNA therapeutics design[41]. All but one
94 guide enabled cleavage with efficiencies close to those observed in the other two tested
95 mRNAs (between 71% to 89%); the outlier, guide 95.2, only cleaved ~ 50% of the
96 substrate, possibly due to local secondary structures that were not fully resolved under
97 the conditions tested.

98 To assess the possibility of off-target cleavage by MpaAgo, we selected guides
99 targeting sequences in Fluc RNA and used them to target pSG90 RNA. We did not
100 detect cleavage, whether in the presence of guides (Fig. S2), further corroborating the
101 highly specific nature of cleavage. Previous work reported that guide length may affect
102 cleavage efficiency on short RNA substrates[37]. We repeated cleavage of Fluc IVT RNA
103 with MpaAgo using 18 nt DNA guides and found similar cleavage efficiencies compared
104 to that using 16 nt guides, with results varying between 61% and complete cleavage
105 (Fig. S3).

106 To expand on the initial characterization of MpaAgo by Li et al.[37], we tested the
107 efficiency of MpaAgo to cleave long RNAs (> 1000 nt) at various temperatures and
108 incubation times (Fig. S4A). We observed very little cleavage of the 1678 nt pSG90 IVT
109 RNA at 4°C even after a 16-hour incubation (Fig. S4B). Increasing the temperature to
110 24°C and 37°C significantly increased cleavage efficiency, with much of the substrate
111 being cut after 30 min incubation at 37°C. Cleavage by MpaAgo was highly effective at
112 50°C, with most of the substrate completely cleaved after 10 min. Importantly, both
113 MpaAgo and a guide were required for specific cleavage as neither MpaAgo nor the
114 guide alone induced cleavage of the substrate RNA (Fig. S4B). MpaAgo-independent
115 degradation of the RNA substrate was observed at 37 or 50°C for 60 min or longer
116 incubation times (Figs. S4A, right panel and S4B), likely due to Mg^{2+} catalyzed
117 hydrolysis of phosphodiester bonds[42].

118 We next tested if the DNA guides could be efficiently removed using DNA
119 exonucleases, which would allow DNA-free downstream processes. *E. coli* exonuclease
120 I, which is a 3'-5' exonuclease with strong preference for single stranded DNA, readily
121 degraded most of the DNA guide from the pAgo reaction (Fig. S5, lane 2). We
122 hypothesize that the small amount of remaining guide may be bound to and thus
123 protected by the MpaAgo protein.
124
125 **Multiplexed cleavage of mRNA**
126 After confirming that pAgos specifically and efficiently cleave RNAs longer than
127 1000 nt, we proceeded to investigate whether MpaAgo could generate the
128 corresponding cleavage fragments in a single reaction when provided with a pool of
129 guides targeting multiple locations along an RNA (Fig. 2A). Consistent with the single
130 cleavage reactions shown in Fig. 1A, incubating MpaAgo with two guides (90.1 and
131 90.2) resulted in specific cleavage of the full-length pSG90 RNA at two individual sites
132 (Fig. 2B). The length of the resulting ~100 nt cleavage fragment (Fig. 2B, lane 4) is
133 consistent with the distance between the target sequences of the two guides. To
134 completely cleave the full-length Fluc RNA into unique 72 nt fragments (plus a 29 nt 5'
135 fragment and an 81 nt 3' fragment), we combined 24 16 nt DNA guides in a single
136 reaction. Using a ratio of substrate to enzyme to total guide pool of 0.1:1:1, complete
137 cleavage of Fluc IVT RNA was achieved (Fig. 2C, experiment 2). However, several
138 fragments of sizes >72 nt were still visible, suggesting that not all guides enabled
139 complete cleavage of their respective target sequences. The addition of 0.5% bovine
140 serum albumin (BSA) to the reaction enhanced cleavage efficiency, collapsing the
141 banding pattern to only three bands besides the unique 5' and 3' end fragments: the
142 desired 72 nt fragments, one prominent band running at 144 nt, and one faint fragment
143 with a size of ~ 220 nt (Fig. 2C, experiment 4). The 144 nt and 220 nt bands likely
144 represent fragments with one or two missing cleavages, indicating that cleavage was
145 still incomplete. We then tested additional supplements to further increase cleavage
146 efficiency. In the absence of BSA, the addition of an 1x enhancer mix containing 0.5 M
147 betaine, 20 mM potassium glutamate, 20% glycerol, and 5% PEG 3350 to the reactions

148 resulted in a similar fragment distribution as did the addition of 0.5% BSA (Fig. 2C,
149 experiment 5). Combining the enhancer mix with 0.5% BSA resulted in the complete
150 cleavage of Fluc mRNA into the programmed RNA fragment sizes (Fig. 2C, experiment
151 3). Cleaved fragments from the reactions containing the guide pool (experiments 2-5)
152 were submitted to LC-MS/MS analysis, indicating sequence coverages between 79 and
153 88% (Fig. 2D and Fig S6). Interestingly, even the reaction without additives that showed
154 only partial cleavage resulted in 79.2% Fluc mRNA sequence coverage (Fig. 2D and
155 Fig. S6, experiment 2), suggesting that complete digestion of the substrate mRNA may
156 not be a prerequisite for high mapping coverage.

157 Recent data suggest that MpaAgo can also use longer DNA guides to cleave
158 RNA[37]. We thus decided to use 18 nt guides to test if longer guides could increase the
159 specificity of MpaAgo targeting and cleavage. While the 16 nt guides were selected to
160 generate uniform 72 nt RNA fragments, the 18 nt guides were designed to generate
161 laddering RNA fragments ranging from 69 to 81 nt and thus simplify oligonucleotide
162 analysis by LC-MS/MS. Under conditions similar to those used with the 16 nt guides,
163 Fluc and pSG90 IVT RNAs were incubated with MpaAgo and their respective 18 nt
164 guide pools (Fig. S7A). Consistently, the addition of the enhancer mix significantly
165 increased RNA site-specific cleavage, collapsing most of the RNA fragment sizes to
166 around 60-80 nt (Fig. S7A, compare experiments 2 and 3, and experiments 5 and 6).
167 Sequence coverage for pSG90 and Fluc mRNAs ranged from 78 to 95%, based on LC-
168 MS/MS analysis (Figs. S7B and S7C).

169 To assess whether an RNA modification commonly used in therapeutic RNAs
170 affect MpaAgo cleavage accuracy and efficiency, we incubated it with a Fluc IVT RNA in
171 which all uridines were replaced with *N*1-methylpseudouridine ($m^1\Psi$) and the same 18
172 nt guide pool as above. Gel electrophoresis revealed partially cleaved higher molecular
173 weight fragments even in the presence of the enhancer mix (Fig. S8A), suggesting that
174 $m^1\Psi$ may affect the cleavage efficiency. Even though cleavage of the fully $m^1\Psi$-
175 modified Fluc was not complete, the ensemble of identified cleavage products was
176 sufficient to generate RNA mapping coverages of around 77% (without enhancer mix)
177 and 86% (with enhancer mix), as determined by LC-MS/MS analysis (Figs. S8B and

178 S8C), which were only marginally lower than those of unmodified Fluc (78 and 95%,
179 respectively).
180 Overall, these data suggest that MpaAgo can be combined with multiple guides
181 in a single reaction to cleave long RNA substrates into fragments of defined sizes,
182 effectively reducing the complexity of the fragment pool (compared to non-specific RNA
183 chemical cleavage or commonly used RNases with short recognition motifs) and
184 enabling high sequence mapping coverage using oligonucleotide LC-MS/MS analysis.
185 We next investigated whether pooled guide DNAs could be employed to
186 simultaneously target multiple RNA species in a one-pot reaction. The resulting
187 cleavage products then serve as species-specific molecular fingerprints, which can be
188 detected by LC-MS/MS to include or exclude RNA species. In reactions containing Fluc
189 or pSG90 IVT RNA—individually or in combination—we introduced Mpa Ago along with
190 a guide set designed to produce three distinct 72 nt fragments from Fluc and a single
191 100 nt fragment from pSG90 (Fig. S9A and S9B). Following cleavage, the reactions
192 were analyzed by LC-MS/MS. In reactions containing only one RNA species, the
193 corresponding target fragments from either Fluc (Fig. S9C) or pSG90 (Fig. S9D) were
194 successfully enriched and identified over unassigned Ago-independent background
195 fragments. Notably, in the reaction containing both RNA species, specific fragments
196 derived from both Fluc and pSG90 were identified (Fig. S9E), indicating that Mpa Ago in
197 combination with multiplexed guide sets enables precise RNA fingerprinting and thus
198 identification of specific species in mixed RNA populations.
199
200 **Generation of custom RNA ladders using pAgos**
201 The ability of pAgos to cleave a long RNA substrate into fragments of
202 predetermined lengths defined by sequence-specific guides opens up the possibility of
203 generating custom RNA ladders containing fragments of desired lengths. To this end,
204 we synthesized a 1576 nt IVT RNA featuring six unique sequences of lengths ranging
205 from 56 to 514 nt that were separated by a specific 20 nt sequence (5'-
206 …CCUACCGUUAAUGACAGGUC… -3', Fig. S10A). A single guide targeting this 20 nt
207 region enabled simultaneous MpaAgo-mediated cleavage at sites between the adjacent

208 sequences, releasing the six sequences from the parental RNA, thus generating a set of
209 fragments with pre-defined lengths. Like in the reactions with multiplexed guides, the
210 addition of the enhancer mix increased the cleavage efficiency and resulted in near
211 complete cleavage of the substrate into a clean and precise RNA ladder, as shown on a
212 denaturing 6% TBE-urea gel (Fig. S10B).
213
214 **RNA 5' cap analysis using MpaAgo**
215 The *N7*-methyl guanosine cap structure at the 5' end of eukaryotic mRNAs is
216 important for nuclear export, stability, and translation of mRNA *in situ*. Determining the
217 efficiency of mRNA 5' capping is an essential quality control step in modern mRNA
218 vaccine/therapeutics manufacturing[43-45]. We sought to investigate whether pAgos could
219 be favorably deployed for mRNA 5' cap analysis. Capillary electrophoresis (CE) was
220 used to assess cleavage efficiency and determine if pAgos could be programmed to
221 cleave near the 5' end of an RNA. A 5'-FAM labeled synthetic 33 nt oligoribonucleotide
222 with a sequence representing the 5' UTR sequence of Fluc mRNA was incubated with
223 MpaAgo, and with one of four guides designed to induce cleavage 20 nt downstream of
224 the 5' end with either a complementary (g1A) or a non-complementary (g1C, g1G, g1T)
225 5'-most nucleotide (Fig. S11A). We found that MpaAgo efficiently and precisely cleaved
226 at the intended site, regardless of the identity of the 5' nucleotide, resulting in the
227 expected 20 nt cleavage fragment (Fig. S11B).
228 Next, we extended this approach to full-length mRNAs. To facilitate capping
229 efficiency testing in a straightforward and cost-effective gel-based assay, we designed
230 guides that specifically targeted a site either 29 nt (Fluc mRNA) or 30 nt (pSG90 mRNA)
231 downstream of their 5' end (Fig. 3A). In both cases, the capped and un-capped
232 cleavage products showed sufficient difference in mobility on a 15% denaturing
233 polyacrylamide gel to observe successful capping (Figs. 3B and 3C).
234 To gain more detailed insight into the nature of the cap structure and estimate
235 the capping efficiency, we turned to LC-MS/MS for the analysis of MpaAgo-mediated
236 cleavage products. We targeted the 5' Fluc-UTR using three distinct guides designed to
237 generate 29 nt (guide Fluc_A1), 26 nt (guide Fluc_A1.2), and 32 nt (guide D891) 5'

238 fragments, respectively. We observed precise Fluc 5' cleavage, producing fragments of
239 the expected lengths 29-mer (90%), 26-mer (87%) and 32-mer (73%) (Fig. S12A).
240 Some low levels of MpaAgo- and guide-independent 5 and 12 nt fragments were also
241 detected (6-20%), which likely represent abortive transcripts (Fig. S12B). The cleavage
242 of the pSG90 5' UTR, too, was highly precise, predominantly yielding the intended 30 nt
243 (D831 guide, >92%) or 21 nt (D892 guide, >94%) 5' fragments (Fig. S12C). Similarly,
244 MpaAgo- and guide-independent 5 and 12 nt fragments were the only other notable
245 fragments detected. As expected, uncapped Fluc mRNA predominantly exhibited 5'
246 triphosphate termini (94%) and fewer diphosphate (5%) ends. In contrast, capped Fluc
247 mRNA was composed exclusively of the Cap-0 (Me^7Gppp) structure (Fig. 3D). Similarly,
248 uncapped pSG90 mRNA consisted of 94% triphosphate and 4% diphosphate 5' ends,
249 whereas capped pSG90 mRNA comprised a mixture of 85% Cap-0, 7% diphosphate,
250 and 3% triphosphate species (Fig. 3E).
251 These data show that MpaAgo can be used to successfully and quickly access
252 the capping status and efficiency – either in a simple, cost-effective gel-based assay or
253 by precise LC-MS/MS analysis.
254
255 **Homogenization of RNA 3' ends and poly(A) tail analysis**
256 Undesired 3' extensions by RNA polymerases are a common byproduct of *in*
257 *vitro* mRNA synthesis using T7 and other RNA polymerases and were first reported in
258 the 1980s[46, 47]. Importantly, these 3' extensions have been reported to negatively impact
259 the efficacy of therapeutic mRNAs[48-50].
260 We envisioned that MpaAgo could be employed to selectively target and cut a
261 specific sequence incorporated into the poly(A) tail of an mRNA to remove unwanted
262 extensions. Such 3' end trimming would generate a mRNA population with homogenous
263 3' ends (Fig. 4A). We utilized a slightly modified version of the poly(A) tail sequence
264 utilized in the BNT162b2 vaccine[51], consisting of a stretch of 30 adenosines, followed by
265 a non-poly(A) sequence (GCATATGACTAAAAAACAT), and 60 terminal adenosines to
266 a 610 nt IVT RNA sequence (pSG95). Guides D758-D761 were designed to induce
267 MpaAgo cleavage in the non-poly(A) sequence (Fig. S13). After cleavage, the reaction

268 products were resolved on a denaturing polyacrylamide gel. We found that guides
269 D758, D760, and D761 enabled the complete cleavage of the full-length substrate at the
270 respective target site, while a small fraction of the substrate remained uncleaved in the
271 reaction with guide D759 (Fig. 4B). These data show that MpaAgo successfully
272 homogenized the 3' ends of IVT products, efficiently cleaving a target embedded in the
273 poly(A) tail.

274 Most current high-resolution methods to access poly(A) tail length and
275 composition include the release of the poly(A) tail by RNase T1, which cleaves 3' of
276 guanosines[52]. However, when we attempted to use RNase T1 to measure poly(A) tail
277 length of *in vitro* transcribed pSG120 mRNA, we found that RNase T1 also cleaved
278 adenosines in a concentration-dependent matter (Fig. S14), necessitating optimization
279 of RNase T1 concentration and digestion conditions for reliable poly(A) tail
280 measurements. Here we show that for a more detailed analysis of poly(A) extensions
281 and/or measurement of the poly(A) tail length using LC-MS/MS, MpaAgo can either be
282 programmed to cleave directly upstream of the poly(A) tail (Fig. 4C) or a target
283 sequence embedded in the tail as described above. The poly(A) tail in these
284 experiments was slightly shortened to accommodate for the resolution of the LC-
285 MS/MS, and to assure full capture of non-templated additions by T7 RNA polymerase
286 without exceeding the range of the LC-MS/MS. MpaAgo was complemented with guides
287 targeting a sequence upstream of the poly(A) tail (D834) or a sequence in the poly(A)
288 tail (D758), resulting in 91 or 56 nt 3' cleavage fragments, respectively (Fig. 4D).
289 Cleavage reactions were performed as described above and the cleavage products
290 analyzed by intact LC-MS/MS. Reactions with either guide allowed for the sequence
291 determination of the 3' cleavage fragments. As expected, in addition to the encoded
292 poly(A) sequence, we observed multiple non-templated addition events by T7 RNA
293 polymerase. In fact, we found that the majority of fragments had one or more additions
294 to the encoded sequence (Fig. 4E). A significant fraction of fragments from both
295 cleavage reactions were found to contain a single additional cytosine, an additional
296 cytosine with one to three adenines, or one to three adenines without cytosine (Tables

297 S1 and S2). These findings agree with what has been reported for non-templated T7
298 RNA polymerase additions[49].
299 These data show that MpaAgo in combination with a guide targeting the poly(A)
300 tail can be used to precisely cleave the 3' end of mRNAs, thus creating mRNA
301 molecules with homogenous ends. The 3' cleavage fragments can be further analyzed
302 by LC-MS/MS for poly(A) tail length measurement and assessment of non-templated
303 additions by RNA polymerases.
304

305 Discussion

306 Although the properties of DNA-targeting pAgos have long been acknowledged
307 and utilized in biotechnological applications, RNA-targeting pAgos have largely been
308 overlooked, likely due to their relative scarcity and limited characterization. In this study,
309 we demonstrate that MpaAgo can serve as a powerful molecular tool, significantly
310 enhancing or simplifying existing analytical workflows, such as RNA sequencing,
311 fingerprinting, 5' cap, and poly(A) tail analysis. Mpa Ago also enables the generation of
312 mRNA populations with homogeneous mRNA 3' ends.
313 We show that pAgos can be programmed with multiplexed guides in a single
314 reaction to specifically and efficiently cleave at multiple sequences in a target mRNA.
315 This suggests that pAgos may be used to address currently unresolved challenges in
316 the analysis, quality control, and sequencing of long RNA molecules and therapeutics,
317 such as self-amplifying RNAs (saRNAs), which exceed 10 kilobases in length. Current
318 methods for mRNA analysis, such as digestion with sequence-specific
319 endoribonucleases like RNase T1 or RNase 4, produce short RNA fragments (typically
320 10-20 nucleotides in length) that are subsequently analyzed by LC-MS/MS[53-56].
321 However, fragmenting mRNAs longer than 5 kilobases into such short fragments results
322 in a complex mixture that is often challenging to deconvolute for full sequence
323 reconstruction and/or modification detection. A possible solution to this problem is to
324 increase the cleavage fragment size to a length that is short enough for mass
325 spectrometry detection analysis, but long enough to reduce the complexity of the
326 oligoribonucleotide pool for RNA sequencing by LC-MS/MS.

327 In our initial experiments aimed at targeting unique sites in Fluc IVT RNA using
328 MpaAgo and multiplexed guides, the guides were designed to produce uniform
329 cleavage fragments with a length of 72 nt. We found that addition of 0.5% BSA slightly
330 increased the sequence coverage of the Fluc mRNA sequence, possibly by reducing
331 non-specific binding of the loaded pAgo complexes to the RNA and other surfaces.
332 Addition of an enhancer mix significantly increased the cleavage efficiency, and thus the
333 controlled fragmentation of the RNA target, increasing the overall mapping coverage.
334 We believe that the crowding agents in the enhancer mix facilitate the targeting of
335 loaded pAgos to their RNA targets by increasing their proximity and thus their ability to
336 interact in solution. Interestingly, adding the enhancer mix in combination with 0.5%
337 BSA led to a reduction of coverage, albeit the gel analysis suggested more efficient
338 cleavage. We hypothesize that the crowding agents increased non-specific binding of
339 BSA to the RNA, potentially blocking access for MpaAgo to its target sites. Thus, BSA
340 may be omitted for MpaAgo cleavage experiments that contain crowding agents (e.g.,
341 as part of the enhancer mix). Another factor potentially responsible for incomplete
342 sequence coverage is the uniform length of the cleavage fragments, as fragments with
343 the same length may not be identifiable/distinguishable due to identical or very similar
344 masses.

345 Off-target cleavage of MpaAgo due to mismatched guide binding or slippage may
346 also negatively affect fragment analysis. We thus set to design guides that a) were
347 comprised of 18 nt instead of 16 nt to increase specificity, and b) induced cleavage into
348 fragments of various lengths, sorted in size-bins ranging from 69 to 81 nt in length, to
349 facilitate data deconvolution. While the band pattern on the gel suggested less efficient
350 cleavage of the Fluc mRNA with the 18 nt guides (compare Fig. 2C, experiment 1 and
351 Fig. S7A, experiment 2), the sequence coverage in reactions without the enhancer mix
352 was comparable (~ 79%). Reactions containing the enhancer mix reproducibly achieved
353 slightly higher coverage (~95%) using 18 nt guides than that of 16 nt guides (~ 88%),
354 suggesting that increasing guide specificity and cleavage of the substrate RNA into
355 binned lengths may be beneficial for RNA sequence analysis. Upon closer inspection of
356 the recovered fragments, we noticed that we were unable to detect fragments spanning

357 Fluc mRNA positions 1056 to 1128 (16 nt guides) and 1064 to 1145 (18 nt guides) in
358 any of our experiments. RNA structure modelling using MXfold2[57] and RNAfold[58] of the
359 respective sequence and flanking regions did not indicate any obvious structural
360 components that may inhibit pAgo binding (data not shown). The presence of the
361 flanking fragments indicate that successful cleavage must have occurred. Sequencing
362 of the IVT template ruled out the possibility of base mutations that could alter the mass
363 of the expected fragments, making them unidentifiable by LC-MS/MS. We hypothesize
364 that the missing fragments may be too similar in mass to other cleavage products that
365 cannot be isolated in the data analysis. We are aware that the RNA sequences tested in
366 this study are shorter than those of saRNAs, and that the maximal number of combined
367 guides tested was 24. However, our results suggest that this application could
368 successfully be used with clinically relevant RNA substrates, especially since full
369 replacement of uridine with $m^1\Psi$, a replacement often found in therapeutic mRNAs to
370 minimize the host immune response, only had a moderate effect on the sequence
371 coverage.

372 pAgos in combination with a smaller pool of multiplexed guides that cleave RNA
373 substrates to generate a unique, characteristic, and identifiable fragment pattern can be
374 used to fingerprint RNAs. This may be useful to confirm the presence of certain RNAs in
375 an RNA mixture (e.g., to analyze the RNA molecule distribution in RNA pools packaged
376 in liquid nanoparticles) or quick detection of a specific target RNA in a biological sample
377 for diagnostic workflows. A similar approach was recently developed using the HD3
378 deoxyribozyme to fragment RNA[59]. Due to its single turnover character, this method
379 requires multiple rounds of cleavage and re-annealing of the HD3 deoxyribozyme pool,
380 which requires up to 24 h total digestion time for complex substrates. This is much
381 slower than the 15 min of cleavage time in the MpaAgo reaction. In addition, the target
382 site choice is limited to a particular set of trinucleotide motifs at which HD3 cleaves, a
383 limitation that does not apply to MpaAgo cleavage.

384 In eukaryotic mRNA, the *N*7-methyl guanosine cap structure is a 5' end
385 modification that is important for nuclear export, RNA stability, and translation. Thus,
386 effective capping of mRNA is an essential part of mRNA-based vaccine and therapeutic

387 synthesis. Current methods of cap analysis combine LC-MS/MS analysis of a defined 5'
388 end fragment of a mRNA that was generated by selective cleavage using either *trans*
389 acting deoxyribozymes[60-62], and ribozymes[63], or a DNA probe-directed approach using
390 either the sequence-nonspecific Ribonuclease H (RNase H)[64], or sequence specific
391 RNases (e.g., RNase 4, MC1, and RNase T1[65, 66]) to cleave the 5' UTR at a specific
392 position and release the cap-containing 5' fragment.

393 Our data show that guided MpaAgo can efficiently release the cap-containing 5'
394 termini of mRNAs, enabling the analysis of mRNA capping efficiency and permitting the
395 determination of the cap structure comparably to other approaches, such as RNase H
396 or sequence-specific RNases. Contrary to non-guided endoribonucleases, pAgos
397 exhibit lower turnover[23, 30], thereby requiring comparatively high enzyme concentrations
398 for effective activity. However, there are significant advantages of using MpaAgo for cap
399 analysis. First, it eliminates the need for a blocking antisense oligo or the
400 presence/incorporation of an endoribonuclease recognition sequence for precise
401 cleavage. Successful 5' fragment generation by sequence-specific endoribonucleases
402 (e.g., RNase T1, RNase 4) requires blocking of all the respective target sites directly
403 downstream of the 5' end by hybridization of a DNA oligo. In addition, the release of the
404 protected fragment is dependent on the presence of a recognition site directly
405 downstream of the duplex. Second, sequence-specific RNases will fragment the entire
406 mRNA downstream of the hybridized probe, in some workflows necessitating the
407 enrichment of the 5' cleavage fragments. Moreover, the additional step of hybridizing of
408 a blocking oligo is not needed with MpaAgo. The use of MpaAgo for 5' end analysis
409 may also allow for the detection of endogenous 5' ends with poorly defined transcription
410 start sites or post-transcriptional modifications[67], in which case the use of a blocking
411 oligo may not be sufficient to protect the heterogeneous 5' ends. Additionally, the
412 transient alignment of the short DNA guide with the RNA target at 50°C may mitigate
413 the influence of RNA structure in the 5' UTR sequence, reducing bias and increasing
414 binding/cleavage efficiency in MpaAgo workflows.

415 A potential caveat of cap analysis with sequence-specific RNases is that it
416 generates RNA/DNA duplexes with a 3'-phosphate and/or 2',3'-cyclic-phosphate

417 overhang. In contrast, the release of single-stranded MpaAgo cleavage products
418 facilitates subsequent 3' end modifications of the fragments, such as fluorescent
419 labeling through fill-in extension using DNA polymerases as in RNase H-based cap
420 analysis methods[64], or enzymatic ligation of the fragments to other nucleic acid
421 sequences.

422 In addition to requiring a significantly shorter reaction time compared to other
423 workflows (15 min vs. 60 min), MpaAgo also facilitates 5' cap analysis by producing
424 cleavage products that do not need to be enriched for LC-MS/MS analysis. In fact, the
425 generation of only two cleavage products (a short 5' fragment and a long 3' fragment)
426 allows for an easy and cheap capping efficiency assessment using PAGE, making this
427 analysis accessible to laboratories without LC-MS/MS capabilities. Recently, a group
428 reported the use of a nucleolytic toxin from a type III toxin/antitoxin system that
429 recognizes a specific 5 nt target sequence to cleave and subsequently analyze 5'
430 mRNA ends for cap detection[68]. Theoretically, mRNA cleavage with Toxin III
431 endoribonucleases also generates only two fragments that enable gel-based capping
432 assessment, and they do not require a DNA guide or oligo for sequence specific
433 cleavage. However, this approach necessitates sequence optimization of the mRNA to
434 remove other potential Toxin III cleavage sites, and – more importantly - a change of the
435 5' UTR sequence to incorporate the target sequence, which may be limiting for certain
436 mRNA constructs. In addition, type III toxins possess a relative specificity rather than an
437 absolute specificity, meaning that they are prone to off-target cleavage at similar
438 sequence motifs[69]. This can result in the generation of additional fragments, which may
439 interfere with cap analysis.

440 One of the shortcomings of using RNase H for cap analysis is its heterogeneous
441 cleavage that results in additional fragments at positions directly upstream or
442 downstream of the desired cleavage site. Optimization of the DNA oligo sequence is
443 often required to reduce off-target cleavage[64]. We show that there is only negligible off-
444 target cleavage by MpaAgo as tested with four different guides on two different mRNAs
445 by CE and LC-MS/MS.

446 We also show that site-directed cleavage by MpaAgo is a superior tool when
447 analyzing RNA 3' ends. The 3' poly(A) tail directly affects mRNA stability and translation
448 efficiency, making it an essential component of native and therapeutic mRNAs. While
449 several low-resolution methods exist that can identify the presence of a poly(A) tail,
450 there are only limited options for detailed analysis of the poly(A) tail length and
451 composition. In addition to next generation sequencing, other high-resolution methods
452 include digestion of the RNA substrate with RNase T1, which cleaves after every
453 guanine, followed by capillary gel electrophoresis or LC-MS/MS[70, 71]. Site-specific
454 removal of the poly(A) tail by MpaAgo for subsequent analysis addresses several
455 shortcomings of digestion with RNase T1. Modern mRNA therapeutics and vaccines
456 incorporate G-containing, non-A islands into the poly(A) tails to increase RNA
457 polymerase accuracy (e.g., Pfizer BNT162b2). Guanines in these sequences will be
458 targeted by RNase T1 and generate a diverse pool of poly(A) fragments which
459 complicates analysis. In addition, we show here that RNase T1 can non-specifically
460 degrade poly(A) regions in a concentration dependent manner. MpaAgo on the other
461 hand can be directed to precisely cleave either the complete poly(A) tail or fragments
462 thereof when targeting the non-A islands. This generates defined cleavage products,
463 which abolishes the need for subsequent purification or enrichment. Furthermore, it
464 simplifies the subsequent analysis by enabling noise-free, single-nucleotide resolution
465 analysis of the poly(A) tail via LC-MS/MS.

466 In addition, MpaAgo uniquely enables 3' end polishing of IVT RNA products to
467 generate RNA populations with homogenous 3' ends. Non-templated addition of
468 nucleotides is a known feature of RNA polymerases *in vitro* that can lead to unwanted
469 consequences (e.g., providing a source for double-stranded RNA (dsRNA) formation).
470 Targeted trimming and thus homogenizing of 3' RNA ends with MpaAgo may prevent
471 and/or significantly reduce the formation of immunogenic dsRNA in RNA manufacturing,
472 addressing a main concern in RNA therapeutics development. Since the MpaAgo
473 enzyme, the short DNA guide, and the cleaved RNA extension can easily be removed
474 from the homogenous RNA pool by proteinase K/DNase I treatment, and/or a sizing
475 column, this workflow could be incorporated into large scale RNA synthesis workflows.

476 Taken together, we show that programmed cleavage of mRNA by MpaAgo
477 enables faster, more precise, and straightforward workflows for multiple important RNA
478 analysis workflows, like 5' capping analysis, RNA sequence/modification mapping, and
479 poly(A) tail analysis – all essential for therapeutic RNA quality assessment. In addition,
480 we show that MpaAgo can be used to generate RNA populations with homogeneous 3'
481 ends, which may help to minimize the presence of immunogenic dsRNA and thus
482 address one of the most critical hurdles in therapeutic RNA production.
483

484 ## Methods

485 ### *In vitro* RNA cleavage assay

486 200 ng of Fluc RNA (~1.8 kb, ~0.37 pmol), a shortened version of the pTsin
487 saRNA (pSG90; ~1.7 kb, ~0.37 pmol), or Epo RNA with a modified sequence (pSG95;
488 ~0.7 kb, ~0.86 pmol), all synthesized using *in vitro* transcription (IVT) (New England
489 Biolabs, #E2040) according to the manufacturer's instructions, were cleaved with
490 MpaAgo in a 10 μL reaction at 50˚C for either 15 minutes (single and double cleavages,
491 1:5 substrate: Ago molar ratio) or 30 minutes (multiplexing, 1:10 substrate: Ago ratio) in
492 1x ThermoPol® reaction buffer (New England Biolabs #B9004S). The Ago:guide molar
493 ratios were 1:5 for single and double cleavages, 1:1 for multiplexing experiments, and
494 1:10 for cleaving polycistronic RNA. DNA guides were pooled using the Echo acoustic
495 liquid handler (Beckman Coulter) and phosphorylated using T4 polynucleotide kinase
496 (New England Biolabs #M0201S) according to the manufacturer's protocols. For
497 multiplexing experiments and when indicated, a 1x enhancer mix containing 0.5 M
498 betaine, 20 mM potassium glutamate, 20% glycerol, and 5% PEG3350 was added to
499 the reactions. BSA was added to 0.5% (v/v) when indicated. Removal of DNA guides
500 was performed by adding 20 U of exonuclease I (New England Biolabs, #M0293),
501 followed by incubation at 37˚C for 15 minutes. Cleavage experiments were stopped by
502 the addition of 0.08 U of proteinase K (New England Biolabs #P8107S) at room
503 temperature for 5-10 minutes. After adding RNA loading dye (New England Biolabs,
504 #B0363), cleaved RNAs were resolved by gel electrophoresis on 6% TBE-urea gels
505 (Thermo Fisher Scientific #EC6265), stained by 0.5x SYBR Gold (Thermo Fisher

506 Scientific #S11494), and analyzed using the Typhoon biomolecule imager (Cytiva) or
507 Odyssey M imager (Licor Bio). For mass spectrometry analysis, reactions were scaled
508 up 10-fold in ThermoPol® reaction buffer (i.e., 2 μg of RNA) at 50˚C for 30 minutes.
509 Cleavage products were then column-purified (New England Biolabs #T2030S) and
510 eluted in 30 μL of nuclease-free water. Purified RNA was subsequently filtered with
511 Ultrafree-MC Centrifugal Filter (Millipore Sigma # UFC30GV0S) for 5 min at 10k x g
512 prior to LC-MS/MS analysis. For RNA fingerprinting, cleavage assays were performed
513 as described above, but with a limited set of guides targeting Fluc IVT RNA and pSG90
514 IVT RNA, generating three 72 nt or one 100 nt RNA species-specific cleavage
515 fragments, respectively. 3.5 pmol of Fluc IVT RNA, 3.5 pmol of pSG90 IVT RNA, or a
516 mix of 1.75 pmol Fluc IVT RNA and 1.75 pmol pSG90 IVT RNA were incubated with
517 17.5 pmol of the guide pool in the presence or absence of 17.5 pmol MpaAgo in 1x
518 ThermoPol® reaction buffer and the enhancer mix for 30 minutes at 50°C. Reactions
519 were stopped by the addition of 0.8 units proteinase K and incubation at 24°C for 10
520 minutes. Following a column cleanup, samples were either ran on a denaturing 6%
521 TBE-urea gel or analyzed by LC-MS/MS.
522
523 **Capping analysis**
524 For 5' mRNA cap analysis experiments, 50 μg (~ 83 pmol) or 25 μg (~ 44 pmol)
525 of Fluc or pSG90 *in vitro* transcribed mRNA, respectively, were initially denatured for 5
526 min at 65°C and immediately put on ice. Both mRNAs were capped using FCE (New
527 England Biolabs #M2081S) according to the manufacturer's manual. The capping
528 reactions were subsequently column purified (New England Biolabs #T2040S). 200 μl
529 reactions containing 3.5 pmol of capped and uncapped Fluc or pSG90 mRNA were then
530 incubated for 15 min at 50°C in 1x ThermoPol® reaction buffer, 30% glycerol, 160 units
531 of Murine RNase Inhibitor (New England Biolabs #M0314S), 67.4 pmol MpaAgo, and
532 66.4 pmol guide (A1: /5Phos/ATCTCCTTCTTAAAGT, A1.2: /5Phos/
533 TCCTTCTTAAAGTTAAAC, D891: /5Phos/ TATATCTCCTTCTTAA targeting Fluc
534 mRNA, or D831: /5Phos/GTCGGCTGTTTGATTC, D892: /5Phos/
535 TTGATTCAATAGTGTG targeting pSG90 mRNA). Reactions were incubated at 50°C.

536 After 15 min, the reactions were put on ice, 120 units of Exonuclease I (New England
537 Biolabs #M0293S) was added, and the reactions incubated at 37°C for 15 min to
538 remove unbound DNA guides. The reactions were stopped by the addition of EDTA to
539 20 mM and incubation at room temperature for 5 min. Finally, reactions were column
540 purified and submitted for LC-MS/MS analysis.
541

542 **3' end homogenization and poly(A) tail analysis**

543 For the analysis of the poly(A) tail composition and length and to homogenize the
544 3' ends of a mRNA population, MpaAgo reactions were scaled up to a 400 μl reaction
545 volume. 67 pmol of *in vitro* transcribed pSG95 (723 nt) or pSG120 (698 nt) mRNAs
546 were incubated with 162 pmol MpaAgo, 800 pmol D758
547 (/5Phos/TATGTTTTTTAGTCATA) or D834 (/5Phos/TTTTTTTATTAGGAGCAG) guides
548 in 1x ThermoPol® reaction buffer with 640 units of Murine RNase Inhibitor for 30 min at
549 50°C. Reactions were stopped by the addition of 1.6 units proteinase K and 10 min
550 incubation at room temperature. Reactions were column purified, followed by
551 enrichment of the poly(A) containing cleavage fragments. The volume of the purified
552 cleavage fragments was adjusted to 50 μl, then 1 volume (50 μl) of high salt buffer (20
553 mM Tris/Cl pH 7.5, 0.5 M $LiCl_2$, 10 mM EDTA) was added. 250 μl of oligo $d(T)_{25}$
554 magnetic beads (New England Biolabs #S1419S) were washed once with 100 μl low
555 salt buffer (20 mM Tris/Cl pH 7.5, 50 mM $LiCl_2$, 10 mM EDTA), and twice with high salt
556 buffer. The RNA was added to the beads and incubated at room temperature on a
557 rotator for 20 min. Bead-bound RNA was washed once with low salt buffer, twice with
558 high salt buffer, and one final time with low salt buffer. To elute the enriched RNA, the
559 beads were incubated with 30 μl of H_2O for 2 min at 50°C in a heat shaker (400 rpm).
560 The eluted RNA was recovered, incubated for 5 min at 65°C, and spun through
561 Ultrafree-MC Centrifugal Filter (Millipore Sigma # UFC30GV0S) for 5 min at 10k x g.
562 The enriched and filtered samples were then subjected to LC-MS/MS analysis.
563

564 **References**

1. Makarova, K.S., Wolf, Y.I., van der Oost, J. & Koonin, E.V. Prokaryotic homologs of Argonaute proteins are predicted to function as key components of a novel system of defense against mobile genetic elements. *Biol Direct* **4**, 29 (2009).
2. Ryazansky, S., Kulbachinskiy, A. & Aravin, A.A. The Expanded Universe of Prokaryotic Argonaute Proteins. *mBio* **9** (2018).
3. Swarts, D.C. et al. The evolutionary journey of Argonaute proteins. *Nat Struct Mol Biol* **21**, 743-753 (2014).
4. Nakanishi, K. Anatomy of RISC: how do small RNAs and chaperones activate Argonaute proteins? *Wiley Interdiscip Rev RNA* **7**, 637-660 (2016).
5. Bobadilla Ugarte, P., Barendse, P. & Swarts, D.C. Argonaute proteins confer immunity in all domains of life. *Curr Opin Microbiol* **74**, 102313 (2023).
6. Joshua-Tor, L. & Hannon, G.J. Ancestral roles of small RNAs: an Ago-centric perspective. *Cold Spring Harb Perspect Biol* **3**, a003772 (2011).
7. Olina, A.V., Kulbachinskiy, A.V., Aravin, A.A. & Esyunina, D.M. Argonaute Proteins and Mechanisms of RNA Interference in Eukaryotes and Prokaryotes. *Biochemistry (Mosc)* **83**, 483-497 (2018).
8. Ozata, D.M., Gainetdinov, I., Zoch, A., O'Carroll, D. & Zamore, P.D. PIWI-interacting RNAs: small RNAs with big functions. *Nat Rev Genet* **20**, 89-108 (2019).
9. Zlotorynski, E. Cell quiescence sends argonaute-2 to transposons. *Nat Rev Mol Cell Biol* **25**, 84 (2024).
10. Underwood, C.J. & Martienssen, R.A. Argonautes team up to silence transposable elements in Arabidopsis. *EMBO J* **34**, 579-580 (2015).
11. Baulcombe, D. RNA silencing in plants. *Nature* **431**, 356-363 (2004).
12. Lisitskaya, L., Aravin, A.A. & Kulbachinskiy, A. DNA interference and beyond: structure and functions of prokaryotic Argonaute proteins. *Nat Commun* **9**, 5165 (2018).
13. Nakanishi, K., Weinberg, D.E., Bartel, D.P. & Patel, D.J. Structure of yeast Argonaute with guide RNA. *Nature* **486**, 368-374 (2012).
14. Kaya, E. et al. A bacterial Argonaute with noncanonical guide RNA specificity. *Proc Natl Acad Sci U S A* **113**, 4057-4062 (2016).
15. Koopal, B., Mutte, S.K. & Swarts, D.C. A long look at short prokaryotic Argonautes. *Trends Cell Biol* **33**, 605-618 (2023).
16. Zaremba, M. et al. Short prokaryotic Argonautes provide defence against incoming mobile genetic elements through NAD(+) depletion. *Nat Microbiol* **7**, 1857-1869 (2022).
17. Swarts, D.C. et al. DNA-guided DNA interference by a prokaryotic Argonaute. *Nature* **507**, 258-261 (2014).
18. Swarts, D.C. et al. Argonaute of the archaeon Pyrococcus furiosus is a DNA-guided nuclease that targets cognate DNA. *Nucleic Acids Res* **43**, 5120-5129 (2015).
19. Kuzmenko, A. et al. DNA targeting and interference by a bacterial Argonaute nuclease. *Nature* **587**, 632-637 (2020).
20. Jolly, S.M. et al. Thermus thermophilus Argonaute Functions in the Completion of DNA Replication. *Cell* **182**, 1545-1559 e1518 (2020).

21. Fu, L. et al. The prokaryotic Argonaute proteins enhance homology sequence-directed recombination in bacteria. *Nucleic Acids Res* **47**, 3568-3579 (2019).
22. Wu, J., Yang, J., Cho, W.C. & Zheng, Y. Argonaute proteins: Structural features, functions and emerging roles. *J Adv Res* **24**, 317-324 (2020).
23. Kuzmenko, A., Yudin, D., Ryazansky, S., Kulbachinskiy, A. & Aravin, A.A. Programmable DNA cleavage by Ago nucleases from mesophilic bacteria Clostridium butyricum and Limnothrix rosea. *Nucleic Acids Res* **47**, 5822-5836 (2019).
24. Olina, A. et al. Genome-wide DNA sampling by Ago nuclease from the cyanobacterium Synechococcus elongatus. *RNA Biol* **17**, 677-688 (2020).
25. Sheng, G. et al. Structure-based cleavage mechanism of Thermus thermophilus Argonaute DNA guide strand-mediated DNA target cleavage. *Proc Natl Acad Sci U S A* **111**, 652-657 (2014).
26. Zander, A. et al. Guide-independent DNA cleavage by archaeal Argonaute from Methanocaldococcus jannaschii. *Nat Microbiol* **2**, 17034 (2017).
27. Kropocheva, E., Kuzmenko, A., Aravin, A.A., Esyunina, D. & Kulbachinskiy, A. A programmable pAgo nuclease with universal guide and target specificity from the mesophilic bacterium Kurthia massiliensis. *Nucleic Acids Res* **49**, 4054-4065 (2021).
28. Liu, Y. et al. A programmable omnipotent Argonaute nuclease from mesophilic bacteria Kurthia massiliensis. *Nucleic Acids Res* **49**, 1597-1608 (2021).
29. Cao, Y. et al. Argonaute proteins from human gastrointestinal bacteria catalyze DNA-guided cleavage of single- and double-stranded DNA at 37 degrees C. *Cell Discov* **5**, 38 (2019).
30. Hegge, J.W. et al. DNA-guided DNA cleavage at moderate temperatures by Clostridium butyricum Argonaute. *Nucleic Acids Res* **47**, 5809-5821 (2019).
31. Agapov, A. et al. Prokaryotic Argonaute nuclease cooperates with co-encoded RNase to acquire guide RNAs and target invader DNA. *Nucleic Acids Res* **52**, 5895-5911 (2024).
32. Liu, Y. et al. Accommodation of Helical Imperfections in Rhodobacter sphaeroides Argonaute Ternary Complexes with Guide RNA and Target DNA. *Cell Rep* **24**, 453-462 (2018).
33. Doxzen, K.W. & Doudna, J.A. DNA recognition by an RNA-guided bacterial Argonaute. *PLoS One* **12**, e0177097 (2017).
34. Miyoshi, T., Ito, K., Murakami, R. & Uchiumi, T. Structural basis for the recognition of guide RNA and target DNA heteroduplex by Argonaute. *Nat Commun* **7**, 11846 (2016).
35. Bastiaanssen, C. et al. RNA-guided RNA silencing by an Asgard archaeal Argonaute. *Nat Commun* **15**, 5499 (2024).
36. Lapinaite, A., Doudna, J.A. & Cate, J.H.D. Programmable RNA recognition using a CRISPR-associated Argonaute. *Proc Natl Acad Sci U S A* **115**, 3368-3373 (2018).
37. Li, W. et al. A programmable pAgo nuclease with RNA target preference from the psychrotolerant bacterium Mucilaginibacter paludis. *Nucleic Acids Res* **50**, 5226-5238 (2022).

38. Lisitskaya, L. et al. Programmable RNA targeting by bacterial Argonaute nucleases with unconventional guide binding and cleavage specificity. *Nat Commun* **13**, 4624 (2022).
39. Graver, B.A., Chakravarty, N. & Solomon, K.V. Prokaryotic Argonautes for in vivo biotechnology and molecular diagnostics. *Trends Biotechnol* **42**, 61-73 (2024).
40. Strauss, E.G., Rice, C.M. & Strauss, J.H. Complete nucleotide sequence of the genomic RNA of Sindbis virus. *Virology* **133**, 92-110 (1984).
41. Vaidyanathan, S. et al. Uridine Depletion and Chemical Modification Increase Cas9 mRNA Activity and Reduce Immunogenicity without HPLC Purification. *Mol Ther Nucleic Acids* **12**, 530-542 (2018).
42. AbouHaidar, M.G. & Ivanov, I.G. Non-enzymatic RNA hydrolysis promoted by the combined catalytic activity of buffers and magnesium ions. *Z Naturforsch C J Biosci* **54**, 542-548 (1999).
43. Ramaswamy, S. et al. Systemic delivery of factor IX messenger RNA for protein replacement therapy. *Proc Natl Acad Sci U S A* **114**, E1941-E1950 (2017).
44. Pardi, N., Hogan, M.J., Porter, F.W. & Weissman, D. mRNA vaccines - a new era in vaccinology. *Nat Rev Drug Discov* **17**, 261-279 (2018).
45. VanBlargan, L.A. et al. An mRNA Vaccine Protects Mice against Multiple Tick-Transmitted Flavivirus Infections. *Cell Rep* **25**, 3382-3392 e3383 (2018).
46. Melton, D.A. et al. Efficient in vitro synthesis of biologically active RNA and RNA hybridization probes from plasmids containing a bacteriophage SP6 promoter. *Nucleic Acids Res* **12**, 7035-7056 (1984).
47. Milligan, J.F., Groebe, D.R., Witherell, G.W. & Uhlenbeck, O.C. Oligoribonucleotide synthesis using T7 RNA polymerase and synthetic DNA templates. *Nucleic Acids Res* **15**, 8783-8798 (1987).
48. Triana-Alonso, F.J., Dabrowski, M., Wadzack, J. & Nierhaus, K.H. Self-coded 3'-extension of run-off transcripts produces aberrant products during in vitro transcription with T7 RNA polymerase. *J Biol Chem* **270**, 6298-6307 (1995).
49. Gholamalipour, Y., Karunanayake Mudiyanselage, A. & Martin, C.T. 3' end additions by T7 RNA polymerase are RNA self-templated, distributive and diverse in character-RNA-Seq analyses. *Nucleic Acids Res* **46**, 9253-9263 (2018).
50. Hur, S. Double-Stranded RNA Sensors and Modulators in Innate Immunity. *Annu Rev Immunol* **37**, 349-375 (2019).
51. Vogel, A.B. et al. BNT162b vaccines protect rhesus macaques from SARS-CoV-2. *Nature* **592**, 283-289 (2021).
52. Brouze, A., Krawczyk, P.S., Dziembowski, A. & Mroczek, S. Measuring the tail: Methods for poly(A) tail profiling. *Wiley Interdiscip Rev RNA* **14**, e1737 (2023).
53. Jiang, T. et al. Oligonucleotide Sequence Mapping of Large Therapeutic mRNAs via Parallel Ribonuclease Digestions and LC-MS/MS. *Anal Chem* **91**, 8500-8506 (2019).
54. Vanhinsbergh, C.J. et al. Characterization and Sequence Mapping of Large RNA and mRNA Therapeutics Using Mass Spectrometry. *Anal Chem* **94**, 7339-7349 (2022).
55. Wolf, E.J. et al. Human RNase 4 improves mRNA sequence characterization by LC-MS/MS. *Nucleic Acids Res* **50**, e106 (2022).

56. Gau, B.C. et al. Oligonucleotide mapping via mass spectrometry to enable comprehensive primary structure characterization of an mRNA vaccine against SARS-CoV-2. *Sci Rep* **13**, 9038 (2023).
57. Sato, K., Akiyama, M. & Sakakibara, Y. RNA secondary structure prediction using deep learning with thermodynamic integration. *Nat Commun* **12**, 941 (2021).
58. Lorenz, R. et al. ViennaRNA Package 2.0. *Algorithms Mol Biol* **6**, 26 (2011).
59. Mutchek, S. et al. Strand-Cleaving Deoxyribozymes Enable the Mid-Down Sequencing of mRNA by Mass Spectrometry with No Front-End Separations. *Anal Chem* **97**, 2972-2980 (2025).
60. Bird, J.G. et al. Highly efficient 5' capping of mitochondrial RNA with NAD(+) and NADH by yeast and human mitochondrial RNA polymerase. *Elife* **7** (2018).
61. Cairns, M.J., King, A. & Sun, L.Q. Optimisation of the 10-23 DNAzyme-substrate pairing interactions enhanced RNA cleavage activity at purine-cytosine target sites. *Nucleic Acids Res* **31**, 2883-2889 (2003).
62. Vlatkovic, I. et al. Ribozyme Assays to Quantify the Capping Efficiency of In Vitro-Transcribed mRNA. *Pharmaceutics* **14** (2022).
63. Inagaki, M. et al. Cap analogs with a hydrophobic photocleavable tag enable facile purification of fully capped mRNA with various cap structures. *Nat Commun* **14**, 2657 (2023).
64. Chan, S.H. et al. RNase H-based analysis of synthetic mRNA 5' cap incorporation. *RNA* **28**, 1144-1155 (2022).
65. Wolf, E.J., Dai, N., Chan, S.H. & Correa, I.R., Jr. Selective Characterization of mRNA 5' End-Capping by DNA Probe-Directed Enrichment with Site-Specific Endoribonucleases. *ACS Pharmacol Transl Sci* **6**, 1692-1702 (2023).
66. Nwokeoji, A.O., Chou, T. & Nwokeoji, E.A. Low Resource Integrated Platform for Production and Analysis of Capped mRNA. *ACS Synth Biol* **12**, 329-339 (2023).
67. Ni, T. et al. A paired-end sequencing strategy to map the complex landscape of transcription initiation. *Nat Methods* **7**, 521-527 (2010).
68. Rothweiler, U. et al. Using nucleolytic toxins as restriction enzymes enables new RNA applications. *Nucleic Acids Res* **52**, e90 (2024).
69. Guegler, C.K. & Laub, M.T. Shutoff of host transcription triggers a toxin-antitoxin system to cleave phage RNA and abort infection. *Mol Cell* **81**, 2361-2373 e2369 (2021).
70. Di Grandi, D. et al. A single-nucleotide resolution capillary gel electrophoresis workflow for poly(A) tail characterization in the development of mRNA therapeutics and vaccines. *J Pharm Biomed Anal* **236**, 115692 (2023).
71. Beverly, M., Hagen, C. & Slack, O. Poly A tail length analysis of in vitro transcribed mRNA by LC-MS. *Anal Bioanal Chem* **410**, 1667-1677 (2018).

Acknowledgements

The authors want to thank Katherine Marks for purifying the pAgo variants tested in this study. We also want to thank Thomas C. Evans Jr. and Eric Cantor for their advice and strong support of this research.

744 **Ethics declarations**

745 At the time of this work, the authors were employed by New England Biolabs,
746 Inc., which funded this work and is the manufacturer of reagents, some of which were
747 used in this manuscript. Even though the authors were employed and funded by New
748 England Biolabs, Inc., this did not detract from the objectivity of data generation or its
749 interpretation.

750

751

752 **Figure legends**

753 **Figure 1. MpaAgo efficiently and specifically cleaves mRNAs.**

754 **(A)** pSG90 IVT RNA (~1.7 kb) was subject to MpaAgo cleavage with single
755 complementary DNA guides in ThermoPol® reaction buffer at 50˚C for 15 minutes. The
756 substrate:Ago molar ratio was 1:5, and the Ago:guide molar ratio was 1:5. 16 nt guides
757 were 5' phosphorylated and were designed for MpaAgo to cleave 100 nt apart from
758 each other. Cleavage products were analyzed on a denaturing 6% TBE-urea gel stained
759 with SYBR Gold. Guide identities and cleavage efficiencies (%) are indicated above the
760 corresponding lanes. **(B)** Fluc IVT RNA (~1.8 kb) was subject to MpaAgo cleavage with
761 single complementary DNA guides. Cleavage reactions were performed under the same
762 conditions as in (A). 16 nt guides for Fluc RNA were also 5' phosphorylated but were
763 designed for MpaAgo to cleave 72 nt apart from each other. Cleavage products were
764 analyzed on a denaturing 6% TBE-urea gel stained with SYBR Gold. Guide identities
765 and cleavage efficiencies (%) were indicated above the corresponding lanes.

766

767 **Figure 2. Guide multiplexing with MpaAgo produces RNA fragments suitable for**
768 **LC-MS/MS analysis.**

769 **(A)** Schematic showing guide multiplexing with pAgo. Guides targeting different regions
770 of an RNA are pooled and used in a single reaction to cleave an RNA into smaller
771 fragments compatible with LC-MS/MS analysis. **(B)** pSG90 IVT RNA (~1.7 kb) was
772 subject to MpaAgo cleavage with single guides (lanes 2 and 3) or two 5' phosphorylated
773 guides in a single reaction (lane 4), at 50˚C for 30 minutes. The substrate:Ago molar

774 ratio was 1:5, and the Ago:guide molar ratio was 1:5. Cleavage products were analyzed
775 on a denaturing 6% TBE-urea gel stained with SYBR Gold. The resulting short cleavage
776 fragments are indicated by asterisks. The target sites for the two guides were 100 nt
777 apart, producing a new 100 nt fragment (black asterisk) when used together. This
778 fragment migrated faster than the 100 nt marker likely due to different buffer
779 compositions or unresolved secondary structure elements. **(C)** Fluc IVT RNA (~1.8 kb)
780 was subjected to MpaAgo cleavage with a pool of 24 5' phosphorylated guides, with or
781 without 0.5% BSA or enhancer mix at 50˚C for 30 minutes as indicated above the gel.
782 The substrate:Ago molar ratio was 1:10, and the Ago:guide molar ratio was 1:1.
783 Cleavage products were analyzed on a denaturing 6% TBE-urea gel stained with SYBR
784 Gold. The distance between target sites of adjacent guides was 72 nt, such that
785 complete cleavage would produce fragments of a uniform 72 nt length in addition to
786 unique 5' and 3' fragments of 29 nt and 81 nt, respectively. Bands ≥ 72 nt represent
787 incomplete cleavage fragments. **(D)** Cleavage products from (C) were analyzed by LC-
788 MS/MS, and the sequence coverage of Fluc RNA (%) are shown in a bar graph.
789 Experimental conditions: 1. no guides; 2. a pool of 24 guides, no additives; 3. 24 guides
790 together with 0.5% BSA and the enhancer mix; 4. 24 guides with 0.5% BSA; and 5. 24
791 guides with the enhancer mix.
792
793 **Figure 3. 5' cap analysis with MpaAgo**
794 **(A)** Schematic of MpaAgo facilitated 5' cap analysis, in which a 5' phosphorylated guide
795 targets MpaAgo cleavage to a site close to the 5' end of a mRNA. Upon substrate
796 release, the resulting fragments are analyzed via LC-MS/MS. **(B)** 5' cleavage fragments
797 (29 nt) of reactions containing Fluc mRNA that was either capped in vitro (+) or
798 uncapped (-) were resolved on a 15% TBE-urea gel. Capped fragments migrate slower
799 in the gel compared to uncapped fragments. The 16 nt guide DNA is indicated. **(C)** 5'
800 cleavage fragments (30 nt) of reactions containing pSG90 mRNA that was either
801 capped in vitro (+) or uncapped (-) were resolved on a 15% TBE-urea gel. **(D)** and **(E)**
802 Heatmap showing the relative intensity of detected 5' fragments starting with a
803 triphosphate (3p), diphosphate (2p), guanosine triphosphate (Gppp), cap 0

804 (1Me7Gppp), N^7,2'-O-dimethylguanosine triphosphate cap (2Me7Gppp) for Fluc mRNA
805 (D), and pSG90 mRNA (E).
806
807 **Figure 4. mRNA 3' end processing by MpaAgo**
808 **(A)** Schematic representation of mRNA 3' end trimming. A non-poly(A) sequence island
809 in the poly(A) tail of a mRNA is targeted and cleaved by MpaAgo, resulting in a mRNA
810 population with homogenized 3' ends, while the 3' fragments can be further analyzed for
811 their composition. **(B)** A 723 nt IVT RNA (pSG95) containing a non-poly(A) island was
812 cleaved at four adjacent sites, using four guides (D758-D761 as indicated above the
813 gel, Fig. S13), and the cleavage products were resolved on a denaturing 6% TBE-urea
814 gel. **(C)** Schema of a reaction where MpaAgo is used to remove the complete poly(A)
815 tail for analysis of the full poly(A) tail by LC-MS/MS. **(D)** Sequences of the 3' region of
816 the pSG120 IVT RNA and two guides (D758, D834). The respective cleavage sites and
817 the lengths of the resulting 3' fragments are indicated. **(E)** LC-MS/MS analysis of the 3'
818 fragments post cleavage using the D758 (left panel) and D834 (right panel) guides. The
819 mass in kDa of the fragments is depicted on the x axis versus the relative intensity on
820 the y axis. The lengths in nt are indicated above each bar.

Figure 1

A

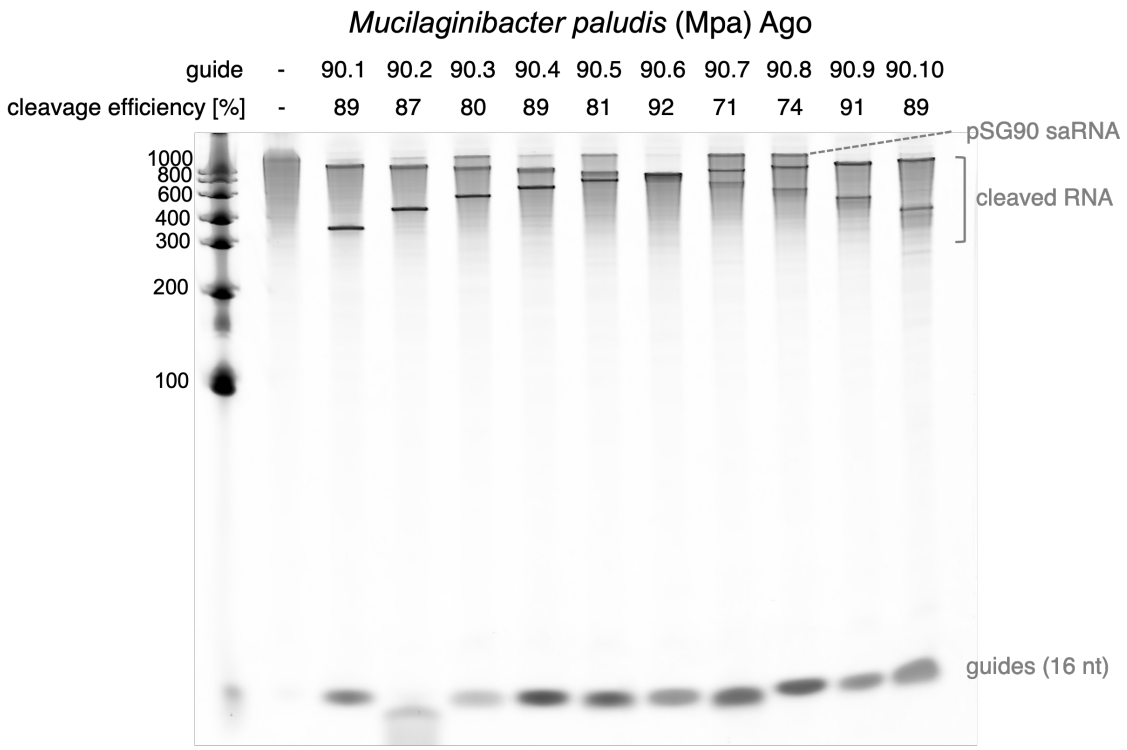
Mucilaginibacter paludis (Mpa) Ago
guide - 90.1 90.2 90.3 90.4 90.5 90.6 90.7 90.8 90.9 90.10
cleavage efficiency [%] - 89 87 80 89 81 92 71 74 91 89
pSG90 saRNA
cleaved RNA
guides (16 nt)
1000
800
600
400
300
200
100

B

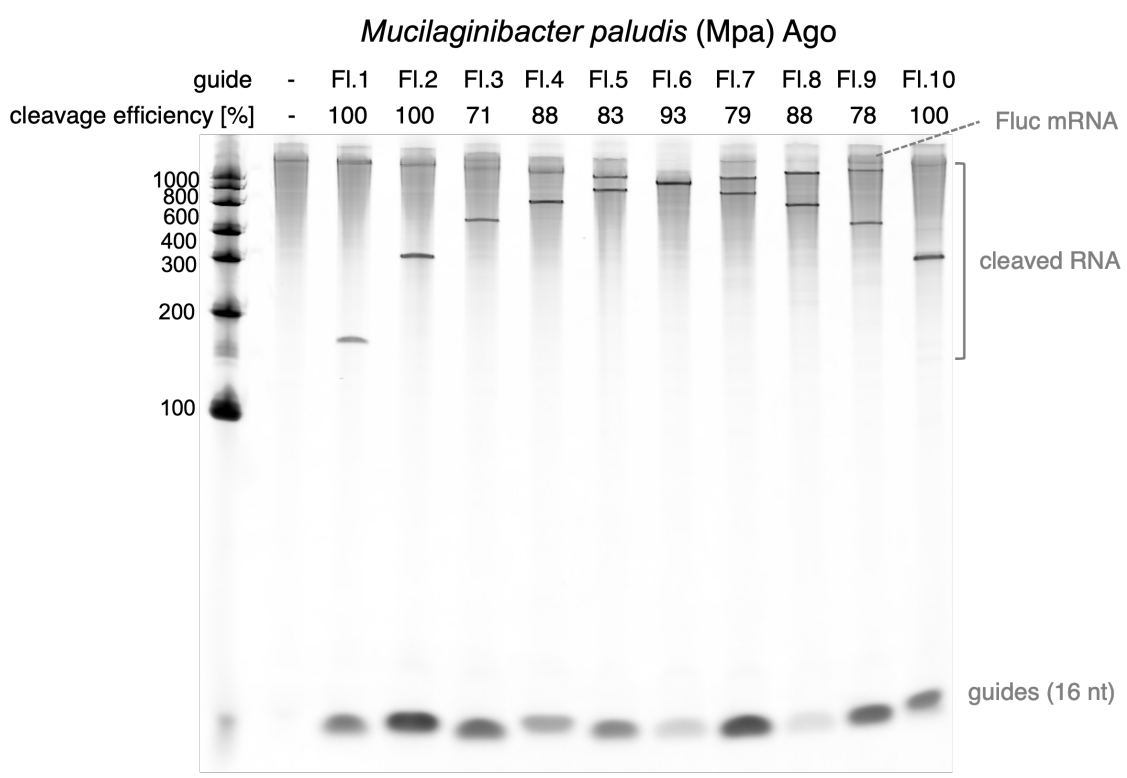
Mucilaginibacter paludis (Mpa) Ago
guide - Fl.1 Fl.2 Fl.3 Fl.4 Fl.5 Fl.6 Fl.7 Fl.8 Fl.9 Fl.10
cleavage efficiency [%] - 100 100 71 88 83 93 79 88 78 100
Fluc mRNA
cleaved RNA
guides (16 nt)
1000
800
600
400
300
200
100

Figure 2

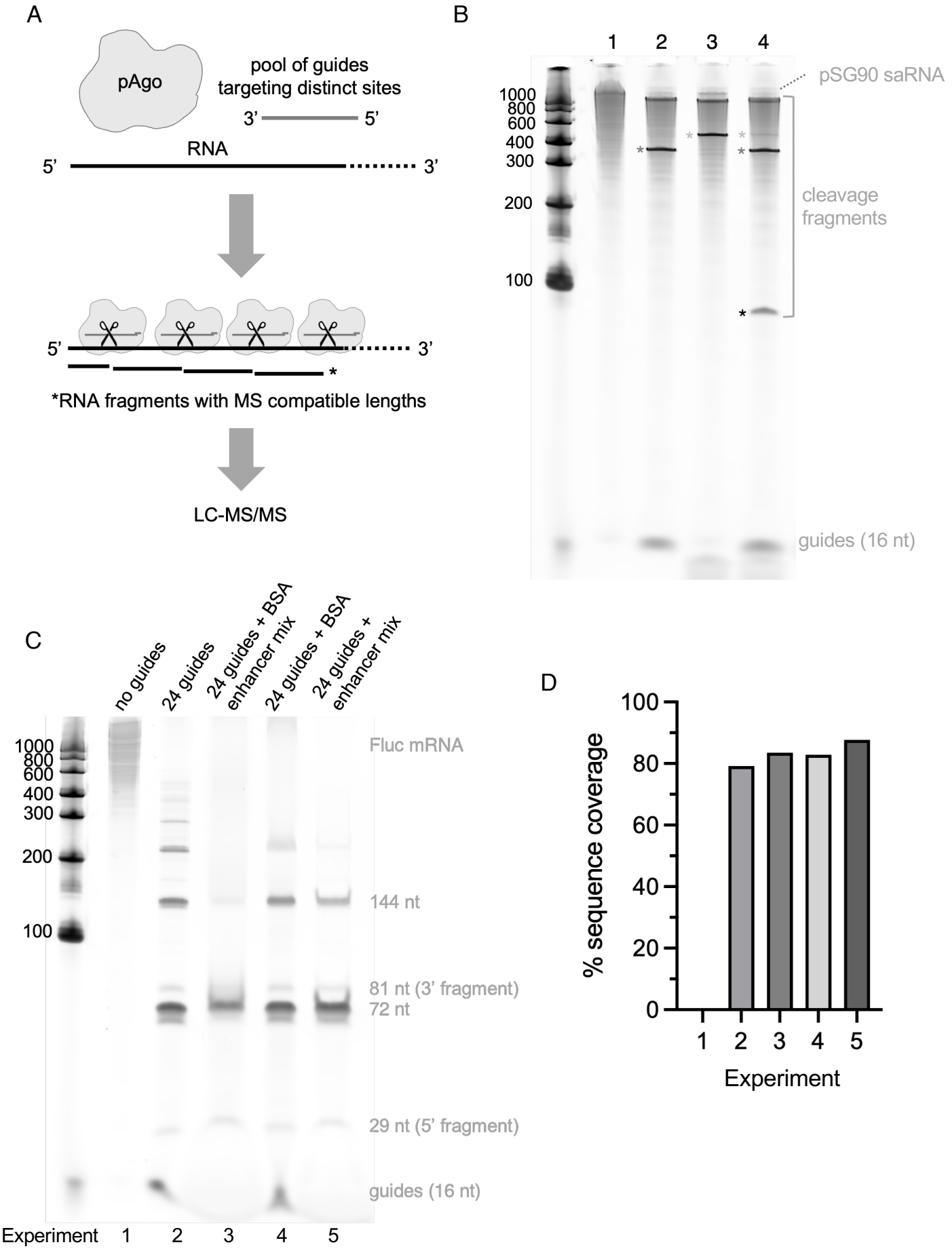
A
pAgo
pool of guides
targeting distinct sites
3'
5'
RNA
5'
3'
5'
3'
*
*RNA fragments with MS compatible lengths
LC-MS/MS
B
1
2
3
4
1000
800
600
400
300
200
100
pSG90 saRNA
cleavage
fragments
guides (16 nt)
C
no guides
24 guides
24 guides + BSA
enhancer mix
24 guides + BSA
24 guides +
enhancer mix
1000
800
600
400
300
200
100
Fluc mRNA
144 nt
81 nt (3' fragment)
72 nt
29 nt (5' fragment)
guides (16 nt)
Experiment
1
2
3
4
5
D
% sequence coverage
100
80
60
40
20
0
1
2
3
4
5
Experiment

Figure 3

A

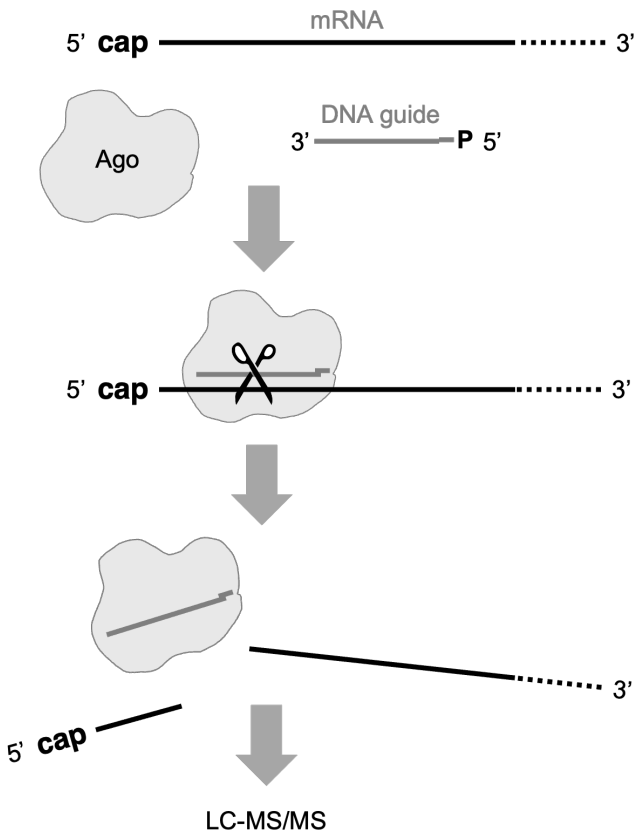

B

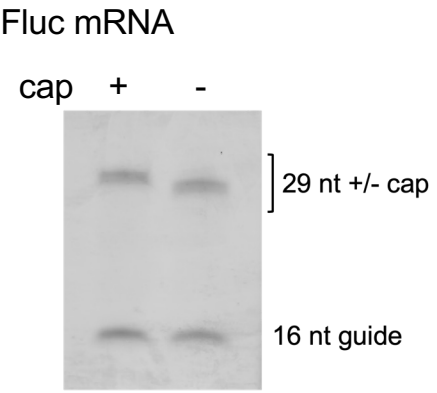

C

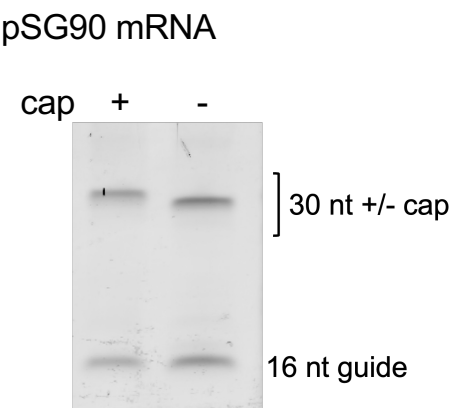

D

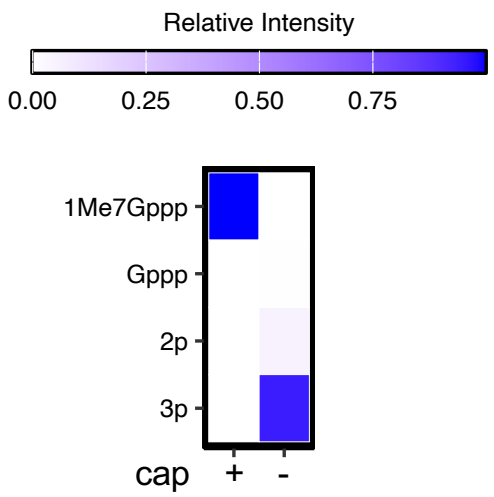

E

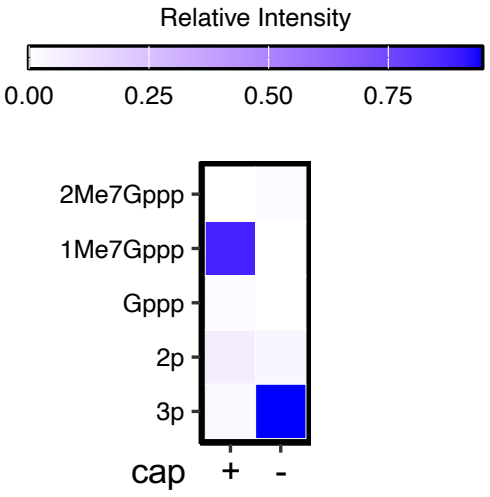

Figure 4

A

pAgo cleavage in poly(A) tail sequence

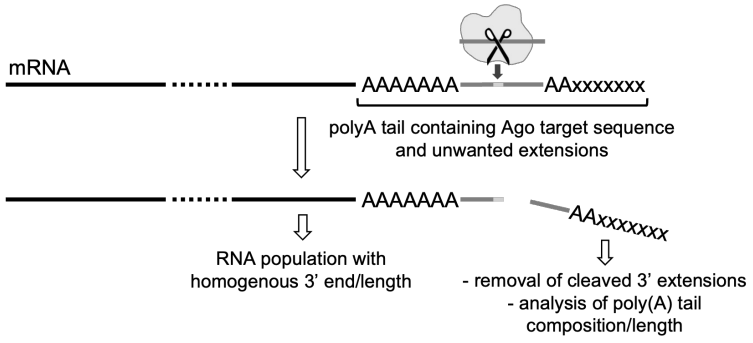

B

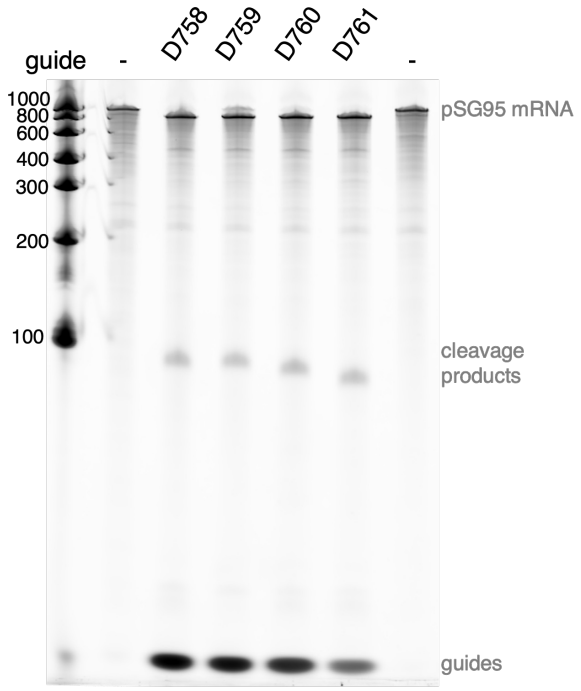

C

pAgo cleavage upstream of poly(A) tail sequence

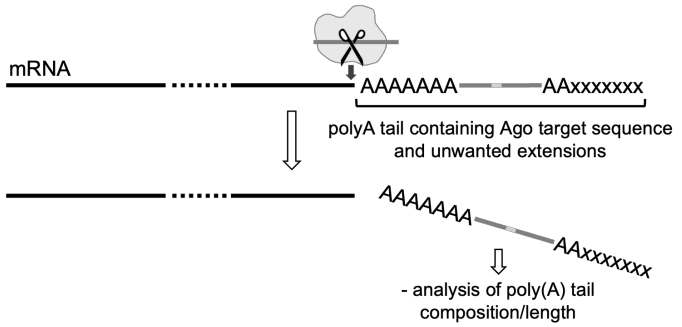

D

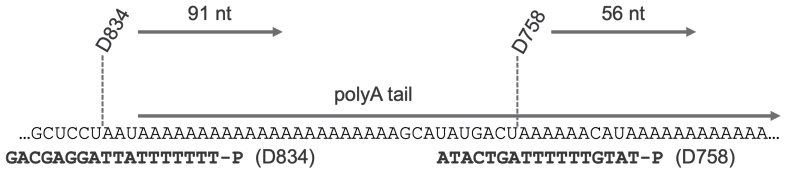

E

RNA fragments after pAgo/D758 cleavage

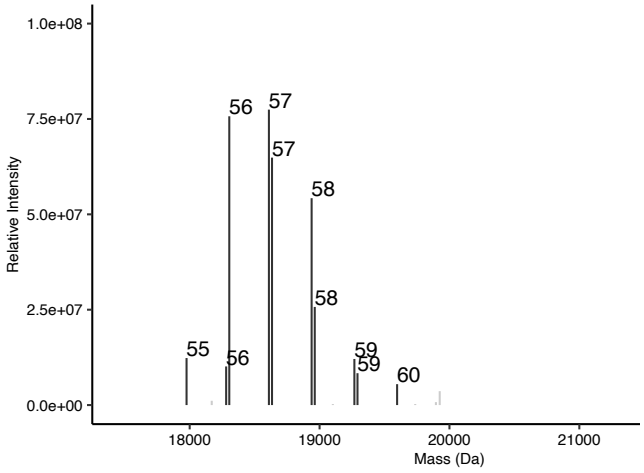
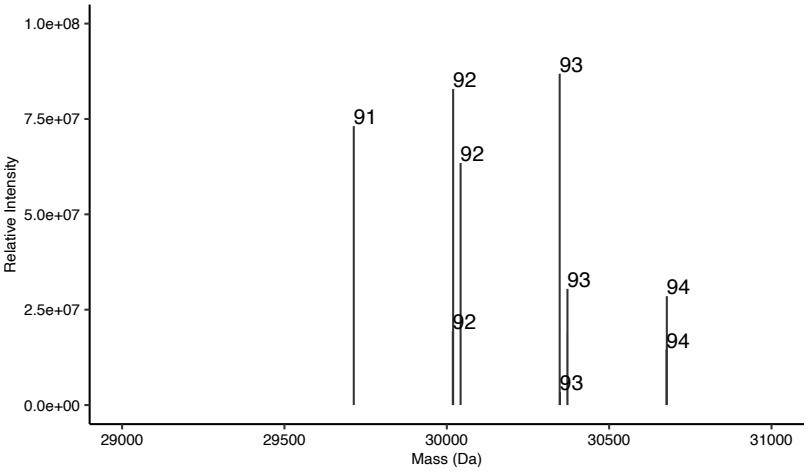
RNA fragments after pAgo/D834 cleavage